Structure-Dynamic Analysis of an Induction Machine Depending on Stator–Housing Coupling

Christoph Schlensok, Michael van der Giet, Mercedes Herranz Gracia, Dirk van Riesen, and Kay Hameyer, *Senior Member, IEEE*

***Abstract*—The estimation and the calculation of the acoustic sound of electric machinery are of particular interest nowadays. Various approaches have been presented, relying either on analytical or on numerical models. The analytical models presented here are based on the electromagnetic-field theory. Numerical models are applied to derive the exciting forces stemming from various sources and effects. The numerical results have to be verified. Hence, they are compared with the physically based analytical results. The radiated noise depends directly on the surface deformation of the machine. Therefore, the analysis is focused on the structure-dynamic vibration. The combined analysis presented here allows for the reduction of vibration and noise, optimizing the coupling of the machine's stator and housing. The studied induction machine's housing is mounted with six spiral-steel springs to the stator. With the presented method, the impact of different numbers of springs is analyzed exemplarily.**

***Index Terms*—Audible noise, deformation, finite-element method (FEM), induction machine, structure dynamics, vibrations.**

I. Introduction

THERE HAVE been several contributions to both the analytical [1]–[3] and numerical [4]–[6] approaches of estimating the radiated noise of electrical machinery. A comparison, as well as a combination, of both methods allows for more reliable predictions and faster improvements of the machine's structure. In this paper, an induction machine (IM) with squirrel-cage rotor is studied by means of analytical and numerical methods. At first, the applied models are introduced. In general, the structure of an IM is not purely cylindrical as the analytical models of [1]–[3] assume. For comparison reasons, different numerical finite-element (FE) models are introduced, and results are analyzed.

Paper IPCSD-07-097, presented at the 2007 IEEE International Electric Machines and Drives Conference, Antalya, Turkey, May 3–5, and approved for publication in the IEEE TRANSACTIONS ON INDUSTRY APPLICATIONS by the Electric Machines Committee of the IEEE Industry Applications Society. Manuscript submitted for review June 16, 2007 and released for publication October 19, 2007.

C. Schlensok is with Bosch Rexroth AG—The Drive and Control Company, 97816 Lohr am Main, Germany (e-mail: Christoph.Schlensok@boschrexroth.de).

M. van der Giet, M. Herranz Gracia, D. van Riesen, and K. Hameyer are with the Institute of Electrical Machines, RWTH Aachen University, 52062 Aachen, Germany (e-mail: Michael.vanderGiet@iem.rwth-aachen.de; Mercedes.HerranzGracia@iem.rwth-aachen.de; Dirk.vanRiesen@iem.rwth-aachen.de; Kay.Hameyer@iem.rwth-aachen.de).

Digital Object Identifier 10.1109/TIA.2008.921440

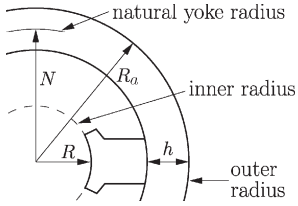

Fig. 1. Simplified analytical model of IM with teeth.

II. Analytical Model

The analytical model [1] is based on the analysis of the force-wave behavior resulting from the normal component of the air-gap flux density B_n depending on space x and time t

$$F_r(x,t) = \frac{B_\mathrm{n}^2(x,t)}{2\mu_0} \tag{1}$$

where μ_0 is the magnetic field constant. $B_\mathrm{n}^2(x,t)$ results from the fundamental and harmonic fields of the stator interacting with the induced fundamental and harmonic fields of the rotor. Three major effects are considered in the analytical model: the fundamental air-gap field, the saturation of the lamination, and the static and dynamic eccentricities. Each harmonic, i.e., each exciting force-wave frequency, results in oscillating space modes along the circumference of the stator at the air gap. The mode number r depends on the interacting field components of stator and rotor.

These force waves excite the structure of the machine, i.e., stator and housing. The analytical model simplifies the machine's structure to a cylindric ring, as shown in Fig. 1. In order to include the effect of slotting, the cylinder-ring model is modified, taking the teeth into account introducing the adjusting factor

$$\Delta = \frac{\text{yoke weight}}{\text{tooth weight} + \text{yoke weight}}. \tag{2}$$

The weight of yoke and teeth is the equivalent to the corresponding cross sections. The eigenfrequency of $r = 0$ reads

$$F_0 = \frac{C_\mathrm{s}}{2\pi \cdot N \cdot \sqrt{\Delta}} \tag{3}$$

with

$$C_\mathrm{s} = \sqrt{\frac{E}{\rho}}. \tag{4}$$

TABLE I
STATIC DEFORMATION FACTORS FOR DIFFERENT MODES r

r	0	1	2	3	4	5	6
$\eta_{r,stat}$	1.0	596.4	35.7	5.0	1.4	0.6	0.3

C_s is calculated by taking the mass density ρ and the Young's modulus E into account. With the analytical model, the deformation magnitude of the analyzed oscillation mode r is estimated on the outer radius of the stator R_a. For this, the static and dynamic deformation factors need to be calculated for an adequate cylinder ring. Since $r = 0$ results in pure tensile stress, the static deformation is calculated to

$$Y_{0,\mathrm{stat}} = \frac{R \cdot N}{E \cdot h} \cdot \sigma(f, r = 0) \tag{5}$$

with the natural yoke radius N, the height of the yoke h, and the inner radius of the stator R. The static deformation for mode number $r \geq 2$ is estimated with

$$Y_{r,\mathrm{stat}} = \frac{R \cdot N}{E \cdot h} \cdot \frac{\sigma}{i^2(r^2-1)^2}, \qquad \text{for} \quad r \geq 2 \tag{6}$$

with

$$i = \left(\frac{1}{2\sqrt{3}}\right) \cdot \left(\frac{h}{N}\right). \tag{7}$$

The static factor as a ratio of $Y_{r,\mathrm{stat}}/Y_{0,\mathrm{stat}}$ reads

$$\eta_{r,\mathrm{stat}} = \frac{12}{(r^2-1)^2} \cdot \left(\frac{N}{h}\right)^2, \qquad \text{for} \quad r \geq 2. \tag{8}$$

Bending forces are generated by $r = 1$. In this special case, the corresponding static factor reads

$$\eta_{1,\mathrm{stat}} = \frac{4}{3} \frac{h \cdot l_\mathrm{Fe}}{N \cdot \left(\frac{d}{L}\right)^4 \cdot L} \tag{9}$$

where l_Fe is the effective stack length, and L is the distance between both bearings. For $r \geq 1$, the factors previously given are multiples of the deformation calculated for $r = 0$. Table I resumes the calculated static deformation factors for the studied IM.

The relative sensitivity of the structure γ is defined as the ratio of the force-wave harmonic f_r and the eigenfrequency F_0. With this and the bending and longitudinal oscillation frequencies f_r^B and f_r^L, respectively, the dynamic factor reads

$$\eta_{r,\mathrm{dyn}} = \frac{r^2 - \gamma^2}{\left[\gamma^2 - \left(\frac{f_r^\mathrm{B}}{F_0}\right)^2\right] \cdot \left[\gamma^2 - \left(\frac{f_r^\mathrm{L}}{F_0}\right)^2\right]}, \qquad \text{for} \quad r \geq 2. \tag{10}$$

In the special case $r = 1$, the lowest bending eigenfrequency is of interest

$$F''_{\mathrm{b}1} = \frac{1}{2\pi}\sqrt{\frac{c''_1}{m''}}. \tag{11}$$

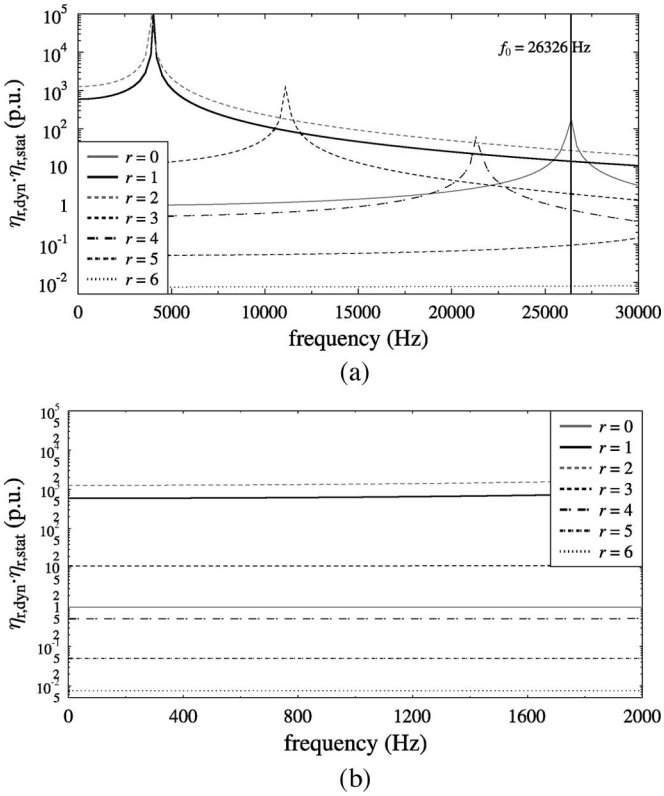

Fig. 2. (a) Resulting factor $\eta_\mathrm{stat} \cdot \eta_\mathrm{dyn}(r)$. (b) Resulting factor $\eta_\mathrm{stat} \cdot \eta_\mathrm{dyn}(r)$ in analyzed frequency range.

For a machine with the shaft diameter d, the spring constant c''_1 and the adequate mass m'' read

$$c''_1 = \frac{3\pi}{4} \cdot E \cdot \left(\frac{d}{L}\right)^4 \cdot L. \tag{12}$$

The adequate mass m'' is calculated by

$$m'' = \rho_\mathrm{Fe} \cdot \left\{ l\left[(2R)^2 - d^2\right] + \frac{1}{2} \cdot L \cdot d^2 \right\} \tag{13}$$

with the mass density ρ_Fe of the rotor. The dynamic deformation factor $r = 1$ reads

$$\eta_{1,\mathrm{dyn}} = \frac{1}{1 - \gamma^2 \cdot \left(\frac{F_0}{F''_{\mathrm{b}1}}\right)^2}. \tag{14}$$

Finally, the overall deformation amplitude is calculated by

$$Y_r = \eta_{r,\mathrm{stat}} \cdot \eta_{r,\mathrm{dynamic}} \cdot Y_{0,\mathrm{stat}}. \tag{15}$$

Fig. 2(a) shows the resulting behavior of the factor $\eta_\mathrm{stat} \cdot \eta_\mathrm{dyn}(r)$. Each mode number r shows a resonance. Due to the small size of the studied IM (800 W), these resonance frequencies are rather high. For $r \geq 4$, they are beyond the human ear's hearing ability. Next to this, the modes $r \geq 3$ produce rather small amplification factors throughout the spectrum. For the analysis of the studied machine, the spectrum is reduced to $f_\mathrm{max} = 1200$ Hz. Here, the entire range of frequencies shows

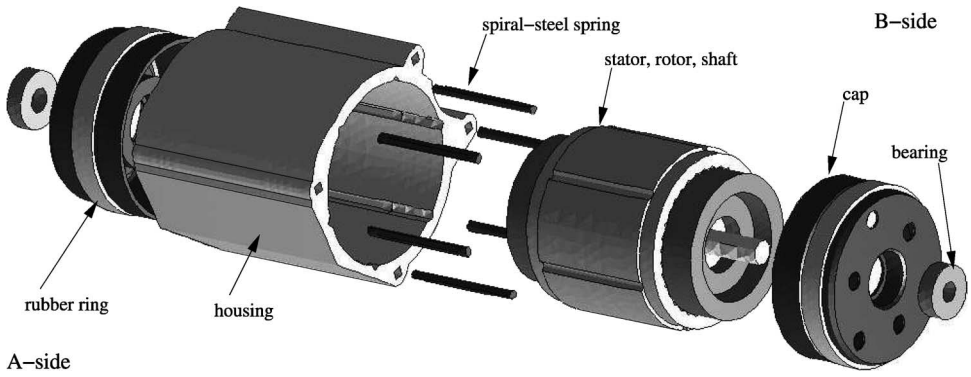

Fig. 3. Mechanical FE model (exploded view).

constant amplifications for all modes, as shown in Fig. 2(b). Therefore, the analysis of the deformation is reduced to small mode numbers $r \leq 10$. In case there are even two modes at the same frequency, the amplification factor decides which of them is important and negligible.

III. Numerical Model

The FE model of the studied IM includes all mechanical parts of the machine, as shown in Fig. 3. This complicated structure of the IM does not correspond exactly to the cylindrical analytical model. The simple model consists of the stator with winding. The numerical model provides the deformation for all nodes of the FE model. After discretizing, the following oscillation equation is obtained:

$$(K + j\omega C - \omega^2 M) \cdot D = F \tag{16}$$

where K is the global stiffness matrix, D is the vector of the node deformation, C is the damping matrix, M is the mass matrix, and F is the excitation force. The exciting frequency f is implemented by $\omega = 2\pi \cdot f$.

In a second step of this paper, the numerical model is modified by applying the entire machine structure shown in Fig. 3. In order to compare the results of both the analytical and numerical models, the analytical model is reapplied for the housing. For this, the deformation of the stator on the outer radius R_a is sampled, depending on the number of spiral-steel springs (Fig. 4). With the deformation samples, the force excitation of the housing is calculated by applying Hooke's law

$$\sigma = E \cdot \epsilon \quad \text{and} \quad \epsilon = \frac{\Delta l}{l} \tag{17}$$

where $l = h$ is the height of the stator yoke, and Δl is the value of the deformation at the location of the spiral-steel spring. The sampling can either be performed with the FE model or the analytical model. After sampling, σ is transformed to the space domain, providing the appearing modes of force excitation $r(\sigma)$. Due to the sampling, aliasing appears, depending on the original mode number. Fig. 5 shows the sampling and resulting mode numbers for $f = 618$ Hz exemplarily. The stator deformation shows a strong mode $r = 6$. In the case of three

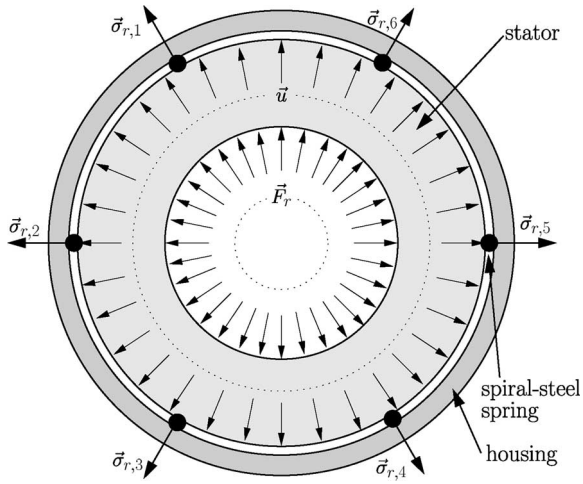

Fig. 4. Sampling of the stator deformation at the location of springs.

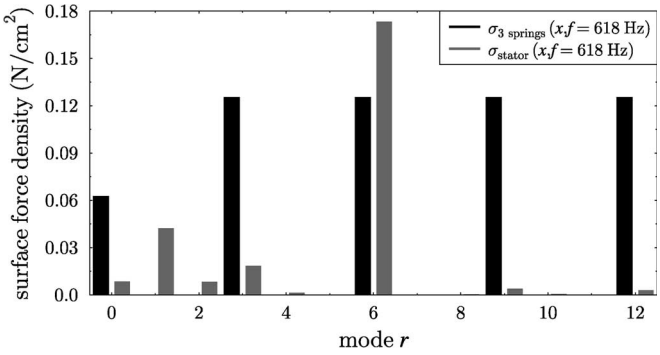

Fig. 5. Aliasing effect changing the exciting modes on the housing.

spiral-steel springs, the most significant mode numbers are $r = 0$ and 3, respectively.

IV. Results

At first, the results of the analytical and numerical models without housing are compared. The deformation is analyzed by separating the modes r. By this, the impact of the mode number can be studied as well. In resuming the deformation values for some selected frequencies, Fig. 6 shows that in the case of two significant modes of the exciting surface-force density, the lower mode number has a significantly higher impact in

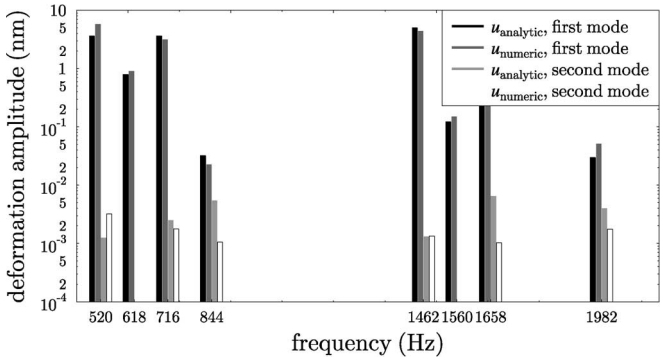

Fig. 6. Comparison of deformation amplitudes for models without housing.

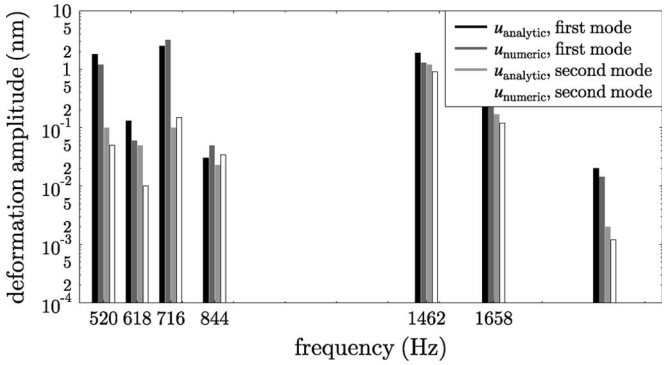

Fig. 7. Comparison of deformation amplitudes for models with housing.

any case. At $f = 844$ Hz, for example, the mode numbers $r = 4$ and 8 occur, the latter having the higher force magnitude. Nevertheless, $r = 4$ reaches the higher deformation amplitude by a factor of 5.8. It can be stated that, in general, if two modes appear, the higher mode can be neglected [1]. The only exception is the case of $r = 0$, which might produce a lower deformation than $r = 1$ and 2. Next to this, Fig. 6 shows a very good agreement of the analytical and numerical models. Since the analytical model has been verified by measurements many times before [1], the numerical model is stated to be reliable.

Finally, the mechanical deformation is simulated for the machine model with the entire detailed structure (Fig. 3). In this way, the impact of different stator-to-housing couplings is analyzed. Three models are studied: two models with three and six spiral-steel springs, respectively, and one with a shrinked stator; an equivalent to an infinite number of springs is studied. Fig. 7 compares the analytical and numerical models with six springs.

Two effects can be stated. First, the housing increases the stiffness of the machine as an additional mass, i.e., the height of the cylinder ring increases (Fig. 1), and it reduces the maximum deformation. Second, the aliasing effect shown in Fig. 5 results in smaller and additional mode numbers producing larger deformation. Both effects are detected in Fig. 7. For example, $f = 844$ Hz shows larger deformation values for the model with housing and six springs. This is due to the fact that the original mode number $r = 8$ is transmitted to $r = 1$ and 2. For $f = 520$ Hz, the maximum deformation at mode $r = 2$ is reduced by more than 50%.

Fig. 8 shows the comparison of the three different stator-to-housing couplings applying the body-sound index L_{M}. It can

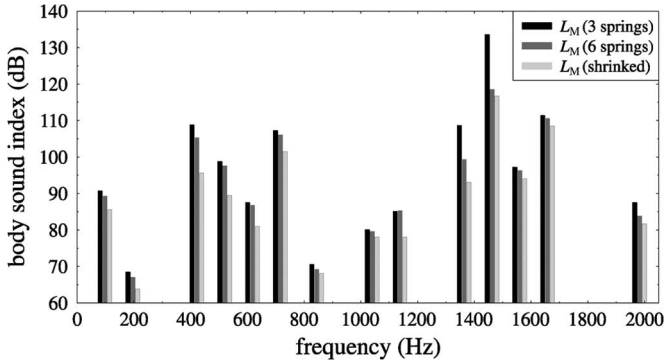

Fig. 8. Comparison of different stator-to-housing couplings.

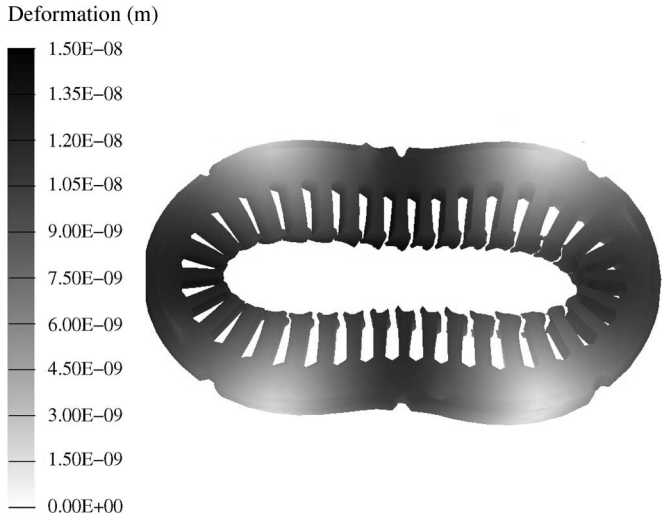

Fig. 9. Deformation of stator at 1462 Hz for a six-pin model.

be stated that for all analyzed frequencies, the shrinked model results in the lowest deformation and vibration. Therefore, this variant will produce the lowest noise radiation. The variant with three springs is the worst and must be avoided.

Large deformation differences can be stated for 1462 Hz (cf. Fig. 8) regarding the models with three or six pins coupling the stator to the housing. For this frequency, deformation and mode results are presented in more detail in the following section.

Figs. 9 and 10 show the deformation of stator and housing for the frequency of 1462 Hz for the model with six pins. A very strong mode 2 deformation can be stated. The same evaluation is performed for the model with three pins. The results are shown in Figs. 11 and 12 for the stator and the housing, respectively. Here, the same force excitation leads to a dominant mode with $r = 1$. Additionally, it can be read from the scale that the maximum deformation amplitude is higher, as was expected from the results in Fig. 8.

Figs. 13 and 14 summarize the deformation modes for the models with six and three pins, respectively. Here, the dominant mode $r = 2$ can be seen for the model with six pins. The model with three pins does not show this mode due to the aliasing effects; here, the deformation stemming from the force excitation in the stator is translated almost entirely to a mode $r = 1$.

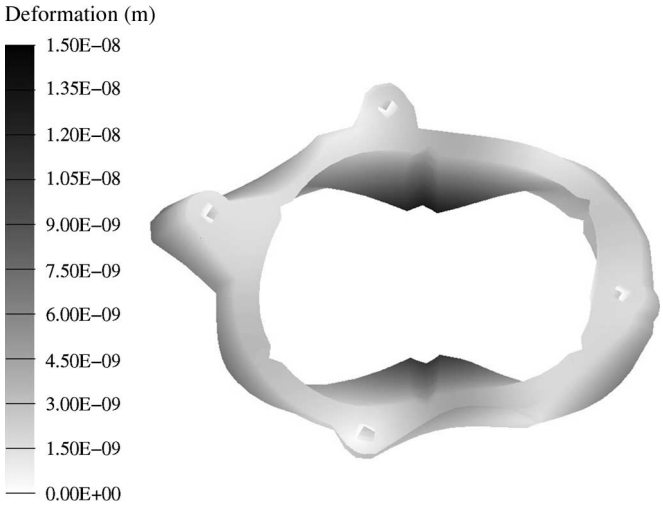

Fig. 10. Deformation of housing at 1462 Hz for a six-pin model.

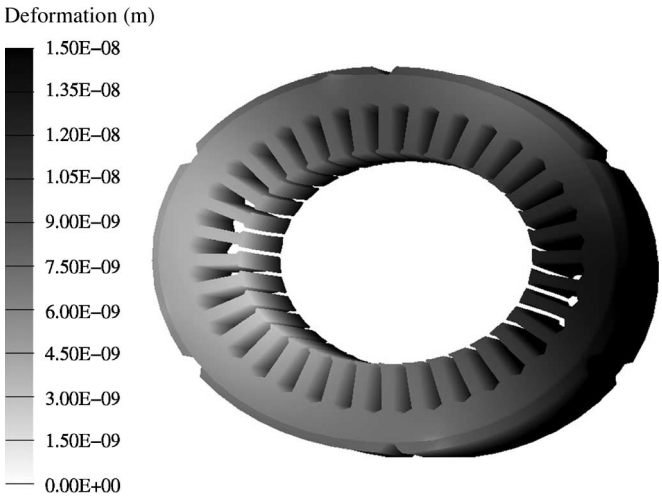

Fig. 11. Deformation of stator at 1462 Hz for a three-pin model.

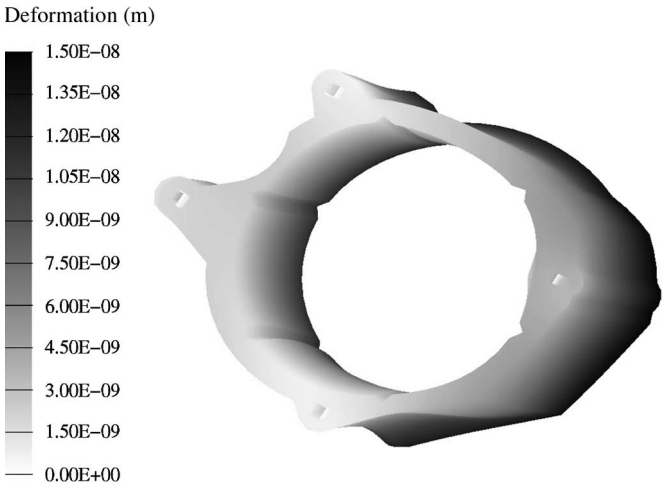

Fig. 12. Deformation of housing at 1462 Hz for a three-pin model.

V. Optimization of the Coupling Between Stator and Housing

In the previous section, it has been demonstrated that shrinking results in the lowest deformation amplitudes. Due to manufacturing reasons, the coupling applying spiral-steel springs is usually preferred. Therefore, a procedure, which determines the optimum number and distribution of the spiral-steel springs, is required.

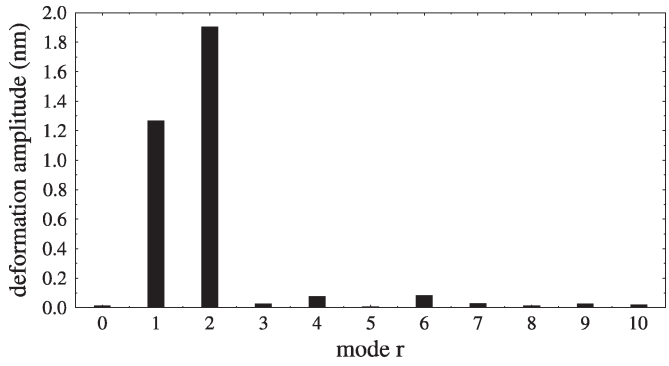

Fig. 13. Modes at 1462 Hz for a six-pin model.

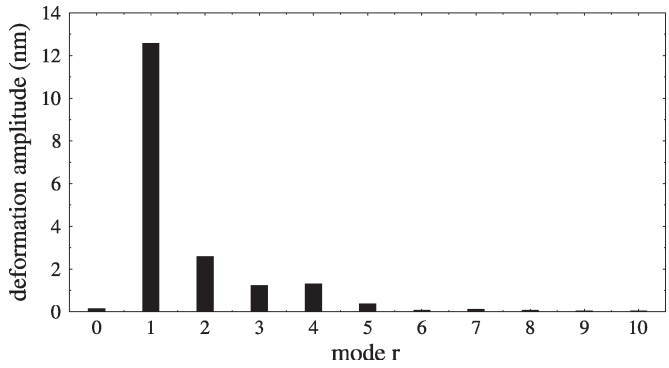

Fig. 14. Modes at 1462 Hz for a three-pin model.

The optimization is performed with regarding the following assumptions:

1) The housing is approximately cylindrical, and the spiral-steel springs are located in the inner radius of the housing.
2) The spiral-steel springs transmit the force excitation from stator to housing at an infinitesimal small (single) spot.
3) The mechanical behavior of the stator is decoupled from the housing's.

The objective of this optimization is the minimization of the sound intensity level L_f for the frequency that generates its maximum value

$$Z = \min\left[\max[L_{I_f}]\right]. \tag{18}$$

The value of the sound intensity level for each frequency is defined as

$$L_{I_f} = 10 \cdot \log \frac{I_f}{I_{\mathrm{s}f}} \tag{19}$$

where $I_{\mathrm{s}f}$ is the threshold value for the human ear of the sound intensity for the frequency f. I_f is the sound intensity generated by the deformation on the surface of the housing with frequency f. For locations at a distance d from the surface of the housing, I_f can be calculated as

$$I_f = k \cdot \frac{u_f^2 \cdot f^4}{d^2} \tag{20}$$

where k is a constant, which depends on the radiation characteristics of the machine, and u_f is the amplitude of the displacement with frequency f. The deformation of the housing is equal to the sum of all significant mode numbers of the deformation amplitude, which is calculated by using the analytical model as follows:

$$u_f = \sum_{r=0}^{r_{\max}} Y_r = \sum_{r=0}^{r_{\max}} \frac{R \cdot N}{E \cdot h} \eta_{r,\mathrm{stat}} \cdot \eta_{r,\mathrm{dyn},f} \cdot \sigma_{r,f} \tag{21}$$

where $\sigma_{r,f}$ is the force excitation for mode number r and frequency f transmitted from the stator to the inner radius of the housing by the spiral-steel springs.

The force excitation at the inner radius of the housing for f is

$$\sigma_f(x) = \sum_{i=1}^{N_{\mathrm{sp}}} \sigma_{i,f} \cdot \delta(x - x_i) \tag{22}$$

where N_{sp} is the number of spiral-steel springs, and $\sigma_{i,f}$ is the force excitation in stator in the position of the spring. It is assumed that it is transmitted without any damping losses to the housing. $\delta(x)$ is the unit impulse function, and x_i is the position along the circumference of each spring. In the case of a symmetrical distribution, it reads

$$x_i = \alpha + i \frac{2\pi}{N_{\mathrm{sp}}} \tag{23}$$

where α is the position of the first spring. $\sigma_f(x)$ can be expressed as a Fourier series with the following coefficients:

$$a_{r,f} = \frac{1}{\pi} \sum_{i=1}^{N_{\mathrm{sp}}} \sigma_{i,f} \cdot \cos(r \cdot x_i) \tag{24}$$

$$b_{r,f} = \frac{1}{\pi} \sum_{i=1}^{N_{\mathrm{sp}}} \sigma_{i,f} \cdot \sin(r \cdot x_i) \tag{25}$$

$$\sigma_{r,f} = \sqrt{a_{r,f}^2 + b_{r,f}^2}. \tag{26}$$

The latter can be used as input data for the calculation of the deformation of the housing (21).

Once the objective function for the optimization is defined, three different approaches according to the optimization parameters are possible.

1) The spiral-steel springs are distributed symmetrically at the stator outer radius, and the influence of the location of the first spring is neglected ($\alpha = 0$). In this case, the only optimization parameter is the number of springs N_{sp}, and the only constraints are that the number of springs should be a natural number and that due to practical reasons, it has to be between 2 and 20.

$$N_{\mathrm{sp}} \in \mathbb{N} \tag{27}$$

$$2 \leq N_{\mathrm{sp}} \leq 20. \tag{28}$$

   In this case, the 1-D optimization can be easily solved by trying all possibilities.

2) The spiral-steel springs are distributed symmetrically at the stator outer radius, and the influence of the position of the first spring α is taken into account. This results in a mixed optimization with two optimization parameters:
   a) the number of spiral-steel springs, with the same constraints as in the previous case;
   b) the position of the first spring α, with the constraints

$$\alpha \in \mathbb{R} \tag{29}$$

$$0 \leq \alpha < \frac{2\pi}{N_{\mathrm{sp}}}. \tag{30}$$

   This mixed 2-D optimization can be solved by using optimization algorithms such as differential evolution [8].

3) The spiral-steel springs are allowed to be distributed unsymmetrically. This results in two types of optimization parameters:
   a) the number of spiral-steel springs, with the known constraints;
   b) the position of each of the springs

$$x_i, \qquad i = 1 \ldots N_{\mathrm{sp}}. \tag{31}$$

   The constraints applying to each of these variables are

$$x_i \in \mathbb{R}^+ \tag{32}$$

$$x_i \neq x_j, \qquad j = 1 \ldots i. \tag{33}$$

   The second constraint forbids that two springs are in the same location.

   In this case, the number of optimization parameters depends on the value of one of these parameters (N_{sp}). Therefore, it is not possible to directly apply optimization algorithms. By taking advantage of the fact that N_{sp} can only take 19 different values, the optimization of the locations of the springs can be performed for each value of N_{sp}, and the global optimum will be the best of the local optima.

The third case is the most general one, and its solution is the global optimum because the possible optima for the first two cases are only a restriction of the possible optima for the third case. This means that it is possible that the optimization of the spring distribution results in a symmetrical distribution such as is assumed in the first two cases. The optimization effort in the third case is, of course, also higher.

VI. Conclusion

This paper has reviewed the analytical theory of [1] and verified the introduced numerical structure-dynamic model. The analysis of the deformational modes shows that small mode numbers have the strongest impact by far. The coupling of housing and stator should either apply shrinking or an adequate number of spiral-steel springs. Moreover, a generalized procedure to optimize this coupling was presented, and the necessary optimization effort was discussed for different assumptions about the coupling. Further results of this optimization will be presented in future works.

REFERENCES

[1] H. Jordan, *Geräuscharme Elektromotoren*. Essen, Germany: Verlag W. Girardet, 1950.

[2] P. L. Timar, *Noise and Vibration on Electrical Machines*. New York: Elsevier, 1998.

[3] S. L. Nau, "Acoustic noise of induction electric motor: Causes and solutions," in *Proc. 2nd Int. Seminar VANEM*, Łódź, Poland, Sep. 2000, pp. 173–178.

[4] O. C. Zienkiewicz and R. L. Taylor, *The Finite Element Method*. London, U.K.: McGraw-Hill, 1989.

[5] J. F. Gieras, C. Wang, and J. C. Lai, *Noise of Polyphase Electric Motors*. Boca Raton, FL: CRC Press, 2005.

[6] L. Vandevelde, J. J. C. Gyselinck, F. Bokose, and J. A. A. Melkebeek, "Vibrations of magnetic origin of switched reluctance motors," *COMPEL*, vol. 22, no. 4, pp. 1009–1020, Nov. 2003.

[7] C. Schlensok, D. van Riesen, T. Küest, and G. Henneberger, "Acoustic simulation of an induction machine with squirrel-cage rotor," *COMPEL*, vol. 25, no. 2, pp. 475–486, Mar. 2006.

[8] K. Hameyer, *Numerical Modelling and Design of Electrical Machines and Devices*. Southampton, U.K.: WIT Press, 1999.

Christoph Schlensok received the M.Sc. degree in electrical engineering and the Ph.D. degree, with a thesis on numeric simulation and optimization of induction machines for power-steering application, from the Faculty of Electrical Engineering and Information Technology, RWTH Aachen University, Aachen, Germany, in 2000 and 2005, respectively.

From 2001 to 2006, he was a Researcher with the Institute of Electrical Machines, RWTH Aachen University. In the beginning of 2007, he moved to industry and is currently a Design Engineer for induction motors, linear motors, and kit motors with Bosch Rexroth AG—The Drive and Control Company, Lohr am Main, Germany. He is a member of the developer team for the finite-element software iMOOSE (www.imoose.de).

Michael van der Giet received the M.Sc. degree in electrical engineering from the Faculty of Electrical Engineering and Information Technology, RWTH Aachen University, Aachen, Germany, in 2004.

Since 2004, he has been a Researcher with the Institute of Electrical Machines, RWTH Aachen University. He is a member of the developer team for the finite-element (FE) software iMOOSE (www.imoose.de). His research fields include the development of FE methods for the simulation of the structure-dynamical behavior of electrical machinery, the numerical simulation and optimization of electrical machines, and the verification of the results by measurements.

Mercedes Herranz Gracia received the M.Sc. degree in power engineering from the Technical University of Catalonia, Barcelona, Spain, in 2004, during a scholarship at the Faculty of Electrical Engineering and Information Technology, RWTH Aachen University, Aachen, Germany.

Since 2004, she has been a Researcher with the Institute of Electrical Machines, RWTH Aachen University. She is a member of the developer team for the finite-element software iMOOSE (www.imoose.de). Her main fields of research interest include numerical design optimization, thermal aspects, and the acoustic behavior of electrical machines, as well as the verification of the numerical results by measurement and testing.

Dirk van Riesen received the M.Sc. degree in electrical engineering and the Ph.D. degree, with a thesis on finite-element (FE) methods for electromagnetic and structure-dynamic simulation of induction furnaces, from RWTH Aachen University, Aachen, Germany, in 1999 and 2004, respectively.

Since 1999, he has been a Researcher with the Institute of Electrical Machines, RWTH Aachen University, where he has been the Chief Engineer since 2004. He is a member of the developer team for the FE software iMOOSE (www.imoose.de). In the beginning of 2008, he moved to industry. He is with Siemens, Bad Neustadt an der Saale, Germany, as Group Manager, Industrial Automation Technologies. His major fields of activity include simulation and measurement of electric machinery and the development of FE software.

Kay Hameyer (M'96–SM'99) received the M.Sc. degree in electrical engineering from the University of Hannover, Hannover, Germany, and the Ph.D. degree from the University of Technology Berlin, Berlin, Germany.

After his university studies, he was with Robert Bosch GmbH, Stuttgart, Germany, as a Design Engineer for permanent-magnet servo motors and electrical energy-supply system components. In 1988, he became a Member of the Staff of the University of Technology Berlin. He was a Full Professor of numerical field computations and electrical machines with the Katholieke Universiteit Leuven, Belgium, until February 2004. In 2005, he was with Poznan University of Technology, Poznan, Poland. He is currently a Full Professor, the Director of the Institute of Electrical Machines, and the holder of the Chair "Electromagnetic Energy Conversion" at RWTH Aachen University, Aachen, Germany, where he has been the Dean of the Faculty of Electrical Engineering and Information Technology since 2007. His research interests include numerical field computation and simulation, design of electrical machines, particularly permanent-magnet excited machines and induction machines, and numerical optimization strategies.